
Design of convergence criterion for fixed stress split iterative scheme for small strain anisotropic poroelastoplasticity coupled with single phase flow

Saumik Dana

University of Southern California
Los Angeles, CA 90007
sdana@usc.edu

Mary F Wheeler

Oden Institute for Computational Engineering and Sciences
University of Texas at Austin
Austin, TX 78712

ABSTRACT

The convergence criterion for the fixed stress split iterative scheme for single phase flow coupled with small strain anisotropic poroelastoplasticity is derived. The analysis is based on studying the equations satisfied by the difference of iterates to show that the iterative scheme is contractive. The contractivity is based on driving a term to as small a value as possible (ideally zero). This condition is rendered as the convergence criterion of the algorithm.

Keywords Staggered solution algorithm · Anisotropic poroelastoplasticity · Coupled flow and mechanics · Contraction map · Convergence criterion

1 Introduction

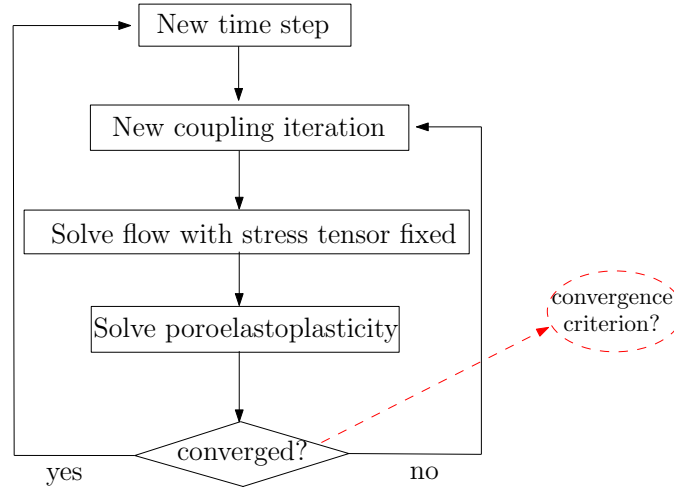


Figure 1: Fixed stress split iterative scheme for anisotropic poroelastoplasticity coupled with single phase flow. Our objective is to use the framework of contraction mapping to design a convergence criterion for the algorithm.

With regard to the numerical simulation of multiphysics phenomena and the advent of modular object oriented programming frameworks, individual physical models are written in separate templates in most mod-

ern code frameworks (Deal.II [1], FEniCS [2], Feel++ [3], FEI (Trilinos) [4], FreeFEM++ [5], libMESH [6], MFEM [7], OOFEM [8] and SOFA [9]). While most of these frameworks are being improved upon on a regular basis, there are specific algorithms designed for specific problems that are developed in-house in research labs. It becomes imperative to collate the features of the open source frameworks with the functionalities of the in-house code developments. In that regard, staggered solution algorithms offer avenues for fast and easy collaboration. These algorithms solve individual physics individually by decoupling the coupled set of partial differential equations and then iterate back and forth in each time step. These algorithms, unlike fully coupled systems, are swift and easy to implement, but they come at the cost of lack of convergence norms. Each staggered solution algorithm needs to be carefully designed with regards to two important aspects: the decoupling constraint and the convergence criterion. The coupling of fluid diffusion with deformation in elasto-plastic porous materials is important from the standpoint of variety of engineering applications not limited to geomaterials [10, 11]. The fixed stress split iterative algorithm has been studied for the coupling of fluid diffusion with deformation in elastic porous material. In this work, we study the fixed stress split algorithm [12–21] for coupling fluid diffusion with deformation in elasto-plastic porous material. We use the framework of a contraction mapping to arrive at the convergence criterion for the algorithm coupling small strain anisotropic poroelastoplasticity with single phase flow. The reader is referred to [22] and [23] for recent work using the framework of contraction mapping. As shown in Figure 1, the flow subproblem is solved with stress tensor fixed followed by the poromechanics subproblem in every coupling iteration at each time step. The coupling iterations are repeated until convergence and Backward Euler is employed for time marching. The analysis is motivated by the results in our previous works as follows

- ✓ In [18], a contraction mapping for two-grid staggered algorithm led to closed form expressions for coarse scale moduli in terms of fine scale data. Here, the flow equations were solved on a fine grid and the isotropic poroelasticity equations were solved on a coarse grid.
- ✓ In [17], a contraction mapping is applied to demonstrate convergence of staggered solution algorithm for anisotropic poroelasticity coupled with single phase flow. The speciality of this algorithm was that the stress tensor is fixed during the flow solve as an extension to the case with isotropic poroelasticity in which the mean stress was fixed during the flow solve.

This paper is divided into the following sections. Model equations with corresponding variational formulations being considered are introduced in Section 2. Convergence criterion is derived in Section 3. A summary of conclusions are presented in Section 4.

2 Model equations and variational statements

We present the equations of the linear flow model and the poromechanics model in this section.

2.1 Linear flow model

Let the boundary $\partial\Omega = \Gamma_D^f \cup \Gamma_N^f$ where Γ_D^f is the Dirichlet boundary and Γ_N^f is the Neumann boundary. The equations are

$$\begin{aligned} \frac{\partial \zeta}{\partial t} + \nabla \cdot \mathbf{z} &= q && \text{(Mass conservation)} \\ \mathbf{z} &= -\frac{\mathbf{K}}{\mu}(\nabla p - \rho_0 \mathbf{g}) = -\boldsymbol{\kappa}(\nabla p - \rho_0 \mathbf{g}) && \text{(Darcy's law)} \\ \rho &= \rho_0(1 + cp) \\ p &= g \text{ on } \Gamma_D^f \times (0, T], \quad \mathbf{z} \cdot \mathbf{n} = 0 \text{ on } \Gamma_N^f \times (0, T] \\ p(\mathbf{x}, 0) &= 0, \quad \rho(\mathbf{x}, 0) = \rho_0(\mathbf{x}), \quad \phi(\mathbf{x}, 0) = \phi_0(\mathbf{x}) && (\forall \mathbf{x} \in \Omega) \end{aligned} \tag{1}$$

where $p : \Omega \times (0, T] \rightarrow \mathbb{R}$ is the fluid pressure, $\mathbf{z} : \Omega \times (0, T] \rightarrow \mathbb{R}^3$ is the fluid flux, ζ is the increment in fluid content¹, q is the source or sink term, \mathbf{K} is the uniformly symmetric positive definite absolute permeability tensor, μ is the fluid viscosity, ϕ is the porosity, $\boldsymbol{\kappa} = \frac{\mathbf{K}}{\mu}$ is a measure of the hydraulic conductivity of the pore fluid, c is the fluid compressibility and $T > 0$ is the time interval.

¹ [24] defines the increment in fluid content as the measure of the amount of fluid which has flowed in and out of a given element attached to the solid frame

2.2 Poromechanics model

The important phenomenological aspects of small strain elastoplasticity are

- ✓ The existence of an elastic domain, i.e. a range of stresses within which the behaviour of the material can be considered as purely elastic, without evolution of permanent (plastic) strains. The elastic domain is delimited by the so-called yield stress. A scalar yield function $\Phi(\boldsymbol{\sigma})$ is introduced. The yield locus is the boundary of the elastic domain where $\Phi(\boldsymbol{\sigma}) = 0$ and the corresponding yield surface is defined as $\mathcal{Y} = \{\boldsymbol{\sigma} | \Phi(\boldsymbol{\sigma}) = 0\}$.
- ✓ If the material is further loaded at the yield stress, then plastic yielding (or plastic flow), i.e. evolution of plastic strains, takes place.

Let the boundary $\partial\Omega = \Gamma_D^p \cup \Gamma_N^p$ where Γ_D^p is the Dirichlet boundary and Γ_N^p is the Neumann boundary. The equations are

$$\begin{aligned}
 \nabla \cdot \boldsymbol{\sigma} + \mathbf{f} &= \mathbf{0} && \text{(Linear momentum balance)} \\
 \mathbf{f} &= \rho\phi\mathbf{g} + \rho_r(1-\phi)\mathbf{g} \\
 \boldsymbol{\epsilon}^e(\mathbf{u}) &= \frac{1}{2}(\nabla\mathbf{u} + (\nabla\mathbf{u})^T) \equiv \boldsymbol{\epsilon}(\mathbf{u}) - \boldsymbol{\epsilon}^p(\mathbf{u}) && \text{(small strain elastoplasticity)} \\
 \boldsymbol{\epsilon}^p &= \gamma \frac{\partial\Phi}{\partial\boldsymbol{\sigma}} && \text{(plastic flow rule)} \\
 \boldsymbol{\sigma} &= \mathbb{D}\boldsymbol{\epsilon}^e - \boldsymbol{\alpha}p \equiv \mathbb{D}(\boldsymbol{\epsilon} - \gamma \frac{\partial\Phi}{\partial\boldsymbol{\sigma}}) - \boldsymbol{\alpha}p && \text{(constitutive law)} \\
 \mathbf{u} &= \mathbf{0} \text{ on } \Gamma_D^p \times [0, T], \quad \boldsymbol{\sigma}^T \mathbf{n} = \mathbf{t} \text{ on } \Gamma_N^p \times [0, T] \\
 \mathbf{u}(\mathbf{x}, 0) &= \mathbf{0} && (\forall \mathbf{x} \in \Omega)
 \end{aligned} \tag{2}$$

where $\mathbf{u} : \Omega \times [0, T] \rightarrow \mathbb{R}^3$ is the solid displacement, ρ_r is the rock density, \mathbf{f} is the body force per unit volume, \mathbf{t} is the traction specified on Γ_N^p , $\boldsymbol{\epsilon}$ is the strain tensor, $\boldsymbol{\epsilon}^e$ and $\boldsymbol{\epsilon}^p$ are the elastic and plastic parts of strain tensor respectively, $\boldsymbol{\sigma}$ is the Cauchy stress tensor, \mathbb{D} is the fourth order symmetric positive definite anisotropic elasticity tensor, $\boldsymbol{\alpha}$ is the Biot tensor and $\gamma \geq 0$ is the plastic multiplier satisfying the complementarity condition

$$\begin{aligned}
 \gamma\Phi &= 0 \\
 \gamma > 0 &\leftrightarrow \Phi = 0 \\
 \gamma = 0 &\leftrightarrow \Phi < 0
 \end{aligned} \tag{3}$$

The inverse of the constitutive law is

$$\boldsymbol{\epsilon}^e = \mathbb{D}^{-1}(\boldsymbol{\sigma} + \boldsymbol{\alpha}p) \equiv \mathbb{D}^{-1}\boldsymbol{\sigma} + \frac{C}{3}\mathbf{B}p \tag{4}$$

where $C(> 0)$ is a generalized Hooke's law constant (see [25]) and \mathbf{B} is the Skempton pore pressure coefficient (see [26]).

2.3 Increment in fluid content

Fluid content is defined as (see [27])

$$\zeta = \frac{1}{M}p + \boldsymbol{\alpha} : \boldsymbol{\epsilon}^e + \phi^p \equiv Cp + \frac{1}{3}C\mathbf{B} : \boldsymbol{\sigma} + \phi^p \tag{5}$$

where $M(> 0)$ is the Biot modulus (see [25, 28]) and ϕ^p is a plastic porosity given by (see [27])

$$\phi^p \equiv \boldsymbol{\beta} : \boldsymbol{\epsilon}^p \tag{6}$$

where $\boldsymbol{\beta}$ is a material parameter.

2.4 Variational statements and spaces used

The problem statement is: find $p_h \in W_h$, $\mathbf{z}_h \in \mathbf{V}_h$ and $\mathbf{u}_h \in \mathbf{U}_h$ such that

$$C(p_h^{k,n+1} - p_h^n, \theta_h)_\Omega + \Delta t(\nabla \cdot \mathbf{z}_h^{k,n+1}, \theta_h)_\Omega + (\phi^{p^{k,n+1}} - \phi^{p^n}, \theta_h)_\Omega$$

$$= \Delta t(q^{n+1}, \theta_h)_\Omega - \frac{C}{3}(\mathbf{B} : (\boldsymbol{\sigma}^{k-1, n+1} - \boldsymbol{\sigma}^n), \theta_h)_\Omega \quad (7)$$

$$(\boldsymbol{\kappa}^{-1} \mathbf{z}_h^{k, n+1}, \mathbf{v}_h)_\Omega = -(g, \mathbf{v}_h \cdot \mathbf{n})_{\Gamma_D^f} + (p_h^{k, n+1}, \nabla \cdot \mathbf{v}_h)_\Omega + (\rho_0 \mathbf{g}, \mathbf{v}_h)_\Omega \quad (8)$$

$$(\mathbf{t}^{n+1}, \mathbf{q}_h)_{\Gamma_N^p} - (\boldsymbol{\sigma}^{k, n+1} : \boldsymbol{\epsilon}^e(\mathbf{q}_h))_\Omega + (\mathbf{f}^{n+1}, \mathbf{q}_h)_\Omega = 0 \quad (9)$$

where the superscript k refers to the coupling iteration count and superscript n refers to time step number and the mixed finite element space $W_h \times \mathbf{V}_h$ and conforming Galerkin space \mathbf{U}_h are given by

$$\begin{aligned} W_h &= \{\theta_h : \theta_h|_E \in P_0(E) \ \forall E \in \mathcal{T}_h\} \\ \mathbf{V}_h &= \{\mathbf{v}_h : \mathbf{v}_h|_E \leftrightarrow \hat{\mathbf{v}}|_{\hat{E}} \in \hat{\mathbf{V}}(\hat{E}) \ \forall E \in \mathcal{T}_h, \ \mathbf{v}_h \cdot \mathbf{n} = 0 \text{ on } \Gamma_N^f\} \\ \mathbf{U}_h &= \{\mathbf{q}_h : \mathbf{q}_h|_E \in Q_1(E) \ \forall E \in \mathcal{T}_h, \ \mathbf{q}_h = \mathbf{0} \text{ on } \Gamma_D^p\} \end{aligned}$$

where P_0 represents the space of constants, Q_1 represents the space of trilinears and the details of $\hat{\mathbf{V}}(\hat{E})$ are given in [17]. The details of (7) and (9) are given in Appendix A.

3 Convergence criterion

To arrive at the convergence criterion, we first arrive at the statement of convergence. We then proceed to simply the convergence criterion by expressing it in terms of computed quantities over every iteration.

3.1 Statement of convergence

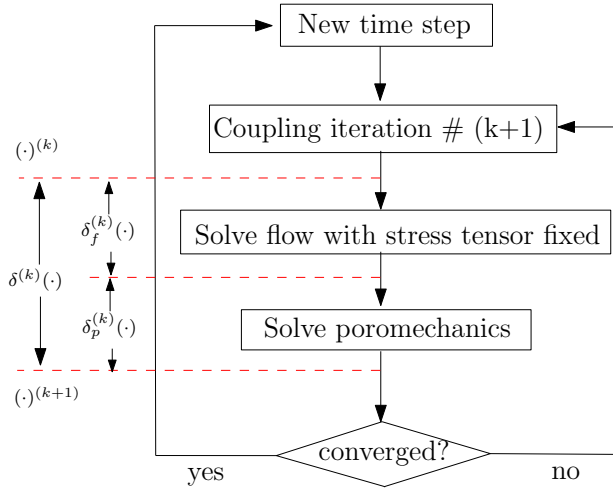


Figure 2: The contraction mapping is in terms of quantities $\delta(\cdot)^{(k)}$ and $\delta(\cdot)_p^{(k)}$.

We follow a procedure similar to that in [17] to arrive at the statement of convergence. As elucidated in Figure 2, we use the notations $\delta_f^{(k)}(\cdot)$ and $\delta_p^{(k)}(\cdot)$ for the change in the quantity (\cdot) during the flow and poromechanics solves respectively over the $(k+1)^{th}$ coupling iteration and $\delta^{(k)}(\cdot)$ for the change in the quantity (\cdot) over the $(k+1)^{th}$ coupling iteration at any time level such that

$$\delta^{(k)}(\cdot) \equiv (\cdot)^{(k+1)} - (\cdot)^k = \delta_f^{(k)}(\cdot) + \delta_p^{(k)}(\cdot)$$

With that in mind, (7)-(9) are written as

$$C(\delta^{(k)} p_h, \theta_h)_\Omega + \Delta t(\nabla \cdot \delta^{(k)} \mathbf{z}_h, \theta_h)_\Omega + (\delta^{(k)} \phi^p, \theta_h)_\Omega = -\frac{C}{3}(\mathbf{B} : \delta^{(k-1)} \boldsymbol{\sigma}, \theta_h)_\Omega \quad (10)$$

$$(\boldsymbol{\kappa}^{-1} \delta^{(k)} \mathbf{z}_h, \mathbf{v}_h)_\Omega = (\delta^{(k)} p_h, \nabla \cdot \mathbf{v}_h)_\Omega \quad (11)$$

$$(\delta^{(k)} \boldsymbol{\sigma} : \boldsymbol{\epsilon}^e(\mathbf{q}_h))_\Omega = 0 \quad (12)$$

Theorem 1. *The fixed stress split scheme is a contraction map with contraction constant $\gamma = \frac{1}{2}$ given by*

$$\begin{aligned} & \|\mathbf{B} : \delta^{(k)} \boldsymbol{\sigma}\|_\Omega^2 + \overbrace{\|\delta^{(k)} p_h\|_\Omega^2}^{\geq 0} + \overbrace{\frac{3}{C} \Delta t \|\boldsymbol{\kappa}^{-1/2} \delta^{(k)} \mathbf{z}_h\|_\Omega^2}^{\geq 0} + \overbrace{\frac{3}{C} (\delta^{(k)} \boldsymbol{\sigma} : \mathbb{D}^{-1} \delta^{(k)} \boldsymbol{\sigma})_\Omega}^{\geq 0} + \overbrace{\frac{3}{2C^2} \|\delta^{(k)} \zeta\|_\Omega^2}^{\geq 0} \\ & - \overbrace{\frac{3}{C^2} \left[\frac{7}{2} \|\delta_p^{(k)} \zeta - \delta_p^{(k)} \phi^p\|_\Omega^2 + \frac{1}{2} \|\delta^{(k)} \phi^p\|_\Omega^2 + \frac{C}{3} (\mathbf{B} : \delta^{(k)} \boldsymbol{\sigma}, \delta^{(k)} \phi^p)_\Omega \right]}^{\rightarrow 0} \leq \gamma \|\mathbf{B} : \delta^{(k-1)} \boldsymbol{\sigma}\|_\Omega^2 \end{aligned}$$

where the term

$$\frac{3}{C^2} \left[\frac{7}{2} \|\delta_p^{(k)} \zeta - \delta_p^{(k)} \phi^p\|_\Omega^2 + \frac{1}{2} \|\delta^{(k)} \phi^p\|_\Omega^2 + \frac{C}{3} (\mathbf{B} : \delta^{(k)} \boldsymbol{\sigma}, \delta^{(k)} \phi^p)_\Omega \right]$$

is driven to a small value by the convergence criterion. The reason behind driving this term to a small value is to minimize the influence of the negativity of the term on the quality of the contraction mapping.

Proof. • **Step 1: Flow equations**

Testing (10) with $\theta_h \equiv \delta^{(k)} p_h$ and (11) with $\mathbf{v}_h \equiv \delta^{(k)} \mathbf{z}_h$, we get

$$C \|\delta^{(k)} p_h\|_\Omega^2 + \Delta t (\nabla \cdot \delta^{(k)} \mathbf{z}_h, \delta^{(k)} p_h)_\Omega + (\delta^{(k)} \phi^p, \delta^{(k)} p_h)_\Omega = -\frac{C}{3} (\mathbf{B} : \delta^{(k-1)} \boldsymbol{\sigma}, \delta^{(k)} p_h)_\Omega \quad (13)$$

$$\|\boldsymbol{\kappa}^{-1/2} \delta^{(k)} \mathbf{z}_h\|_\Omega^2 = (\delta^{(k)} p_h, \nabla \cdot \delta^{(k)} \mathbf{z}_h)_\Omega \quad (14)$$

From (13) and (14), we get

$$C \|\delta^{(k)} p_h\|_\Omega^2 + \Delta t \|\boldsymbol{\kappa}^{-1/2} \delta^{(k)} \mathbf{z}_h\|_\Omega^2 + (\delta^{(k)} \phi^p, \delta^{(k)} p_h)_\Omega = -\frac{C}{3} (\mathbf{B} : \delta^{(k-1)} \boldsymbol{\sigma}, \delta^{(k)} p_h)_\Omega \quad (15)$$

• **Step 2: Poromechanics equations**

Testing (12) with $\mathbf{q}_h \equiv \delta^{(k)} \mathbf{u}_h$, we get

$$(\delta^{(k)} \boldsymbol{\sigma} : \delta^{(k)} \boldsymbol{\epsilon}^e)_\Omega = 0 \quad (16)$$

We now invoke (4) to arrive at $\delta^{(k)} \boldsymbol{\epsilon}^e = \mathbb{D}^{-1} \delta^{(k)} \boldsymbol{\sigma} + \frac{C}{3} \mathbf{B} \delta^{(k)} p_h$. Substituting in (16), we get

$$(\delta^{(k)} \boldsymbol{\sigma} : \mathbb{D}^{-1} \delta^{(k)} \boldsymbol{\sigma})_\Omega + \frac{C}{3} (\mathbf{B} : \delta^{(k)} \boldsymbol{\sigma}, \delta^{(k)} p_h)_\Omega = 0 \quad (17)$$

• **Step 3: Combining flow and poromechanics equations**

Adding (15) and (17), we get

$$\begin{aligned} & C \|\delta^{(k)} p_h\|_\Omega^2 + \Delta t \|\boldsymbol{\kappa}^{-1/2} \delta^{(k)} \mathbf{z}_h\|_\Omega^2 + (\delta^{(k)} \phi^p, \delta^{(k)} p_h)_\Omega + (\delta^{(k)} \boldsymbol{\sigma} : \mathbb{D}^{-1} \delta^{(k)} \boldsymbol{\sigma})_\Omega + \frac{C}{3} (\mathbf{B} : \delta^{(k)} \boldsymbol{\sigma}, \delta^{(k)} p_h)_\Omega \\ & = -\frac{C}{3} (\mathbf{B} : \delta^{(k-1)} \boldsymbol{\sigma}, \delta^{(k)} p_h)_\Omega \end{aligned} \quad (18)$$

• **Step 4: Variation in fluid content**

In lieu of (5), we write

$$\delta^{(k)} \zeta = C \delta^{(k)} p_h + \frac{C}{3} \mathbf{B} : \delta^{(k)} \boldsymbol{\sigma} + \delta^{(k)} \phi^p \quad (19)$$

which can be written as

$$\|\delta^{(k)} \zeta\|_\Omega^2 = C^2 \|\delta^{(k)} p_h\|_\Omega^2 + \frac{C^2}{9} \|\mathbf{B} : \delta^{(k)} \boldsymbol{\sigma}\|_\Omega^2 + \|\delta^{(k)} \phi^p\|_\Omega^2 + \frac{2C^2}{3} (\delta^{(k)} p_h, \mathbf{B} : \delta^{(k)} \boldsymbol{\sigma})_\Omega$$

$$+ \frac{2C}{3}(\mathbf{B} : \delta^{(k)} \boldsymbol{\sigma}, \delta^{(k)} \phi^p)_\Omega + 2C(\delta^{(k)} p_h, \delta^{(k)} \phi^p)_\Omega$$

Dividing throughout by $2C$, we get

$$\begin{aligned} & \frac{1}{2C} \|\delta^{(k)} \zeta\|_\Omega^2 - \frac{C}{2} \|\delta^{(k)} p_h\|_\Omega^2 - \frac{C}{18} \|\mathbf{B} : \delta^{(k)} \boldsymbol{\sigma}\|_\Omega^2 - \frac{1}{2C} \|\delta^{(k)} \phi^p\|_\Omega^2 \\ & - \frac{1}{3}(\mathbf{B} : \delta^{(k)} \boldsymbol{\sigma}, \delta^{(k)} \phi^p)_\Omega = \frac{C}{3}(\mathbf{B} : \delta^{(k)} \boldsymbol{\sigma}, \delta^{(k)} p_h)_\Omega + (\delta^{(k)} \phi^p, \delta^{(k)} p_h)_\Omega \end{aligned} \quad (20)$$

From (18) and (20), we get

$$\begin{aligned} & C \|\delta^{(k)} p_h\|_\Omega^2 + \Delta t \|\boldsymbol{\kappa}^{-1/2} \delta^{(k)} \mathbf{z}_h\|_\Omega^2 + (\delta^{(k)} \boldsymbol{\sigma} : \mathbb{D}^{-1} \delta^{(k)} \boldsymbol{\sigma})_\Omega + \frac{1}{2C} \|\delta^{(k)} \zeta\|_\Omega^2 \\ & - \frac{C}{2} \|\delta^{(k)} p_h\|_\Omega^2 - \frac{C}{18} \|\mathbf{B} : \delta^{(k)} \boldsymbol{\sigma}\|_\Omega^2 - \frac{1}{2C} \|\delta^{(k)} \phi^p\|_\Omega^2 - \frac{1}{3}(\mathbf{B} : \delta^{(k)} \boldsymbol{\sigma}, \delta^{(k)} \phi^p)_\Omega \\ & = -\frac{C}{3}(\mathbf{B} : \delta^{(k-1)} \boldsymbol{\sigma}, \delta^{(k)} p_h)_\Omega \end{aligned} \quad (21)$$

Adding and subtracting $\frac{C}{3} \|\mathbf{B} : \delta^{(k)} \boldsymbol{\sigma}\|_\Omega^2$ to the LHS of (21) results in

$$\begin{aligned} & \frac{C}{3} \|\mathbf{B} : \delta^{(k)} \boldsymbol{\sigma}\|_\Omega^2 + \frac{C}{2} \|\delta^{(k)} p_h\|_\Omega^2 + \Delta t \|\boldsymbol{\kappa}^{-1/2} \delta^{(k)} \mathbf{z}_h\|_\Omega^2 + (\delta^{(k)} \boldsymbol{\sigma} : \mathbb{D}^{-1} \delta^{(k)} \boldsymbol{\sigma})_\Omega \\ & + \frac{1}{2C} \|\delta^{(k)} \zeta\|_\Omega^2 - \frac{7C}{18} \|\mathbf{B} : \delta^{(k)} \boldsymbol{\sigma}\|_\Omega^2 - \frac{1}{2C} \|\delta^{(k)} \phi^p\|_\Omega^2 - \frac{1}{3}(\mathbf{B} : \delta^{(k)} \boldsymbol{\sigma}, \delta^{(k)} \phi^p)_\Omega \\ & = -\frac{C}{3}(\mathbf{B} : \delta^{(k-1)} \boldsymbol{\sigma}, \delta^{(k)} p_h)_\Omega \end{aligned}$$

Multiplying throughout by C results in

$$\begin{aligned} & \frac{C^2}{3} \|\mathbf{B} : \delta^{(k)} \boldsymbol{\sigma}\|_\Omega^2 + \frac{C^2}{2} \|\delta^{(k)} p_h\|_\Omega^2 + C \Delta t \|\boldsymbol{\kappa}^{-1/2} \delta^{(k)} \mathbf{z}_h\|_\Omega^2 + C(\delta^{(k)} \boldsymbol{\sigma} : \mathbb{D}^{-1} \delta^{(k)} \boldsymbol{\sigma})_\Omega \\ & + \frac{1}{2} \|\delta^{(k)} \zeta\|_\Omega^2 - \frac{7C^2}{18} \|\mathbf{B} : \delta^{(k)} \boldsymbol{\sigma}\|_\Omega^2 - \frac{1}{2} \|\delta^{(k)} \phi^p\|_\Omega^2 - \frac{C}{3}(\mathbf{B} : \delta^{(k)} \boldsymbol{\sigma}, \delta^{(k)} \phi^p)_\Omega \\ & = -\frac{C^2}{3}(\mathbf{B} : \delta^{(k-1)} \boldsymbol{\sigma}, \delta^{(k)} p_h)_\Omega \end{aligned} \quad (22)$$

• **Step 5: Invoking the fixed stress constraint**

Using (5) and the fixed stress constraint during the flow solve, we get

$$\delta_f^{(k)} \zeta = C \delta_f^{(k)} p_h + \frac{C}{3} \mathbf{B} : \delta_f^{(k)} \boldsymbol{\sigma} + \delta_f^{(k)} \phi^p$$

Further, since the pore pressure is frozen during the poromechanical solve, we have $\delta_f^{(k)} p_h = \delta^{(k)} p_h$. As a result, we can write

$$\delta_f^{(k)} \zeta = C \delta^{(k)} p_h + \delta_f^{(k)} \phi^p \quad (23)$$

Subtracting (23) from (19), we can write

$$\delta_p^{(k)} \zeta = \frac{C}{3} \mathbf{B} : \delta^{(k)} \boldsymbol{\sigma} + \delta_p^{(k)} \phi^p \quad (24)$$

which implies that

$$\|\delta_p^{(k)} \zeta - \delta_p^{(k)} \phi^p\|_\Omega^2 = \frac{C^2}{9} \|\mathbf{B} : \delta^{(k)} \boldsymbol{\sigma}\|_\Omega^2 \quad (25)$$

Noting (25), we can write (22) as

$$\begin{aligned} & \frac{C^2}{3} \|\mathbf{B} : \delta^{(k)} \boldsymbol{\sigma}\|_{\Omega}^2 + \frac{C^2}{2} \|\delta^{(k)} p_h\|_{\Omega}^2 + C \Delta t \|\boldsymbol{\kappa}^{-1/2} \delta^{(k)} \mathbf{z}_h\|_{\Omega}^2 + C(\delta^{(k)} \boldsymbol{\sigma} : \mathbb{D}^{-1} \delta^{(k)} \boldsymbol{\sigma})_{\Omega} \\ & + \left[\frac{1}{2} \|\delta^{(k)} \zeta\|_{\Omega}^2 - \frac{7}{2} \|\delta_p^{(k)} \zeta - \delta_p^{(k)} \phi^p\|_{\Omega}^2 - \frac{1}{2} \|\delta^{(k)} \phi^p\|_{\Omega}^2 - \frac{C}{3} (\mathbf{B} : \delta^{(k)} \boldsymbol{\sigma}, \delta^{(k)} \phi^p)_{\Omega} \right] \\ & = -\frac{C^2}{3} (\mathbf{B} : \delta^{(k-1)} \boldsymbol{\sigma}, \delta^{(k)} p_h)_{\Omega} \end{aligned} \quad (26)$$

• **Step 6: Invoking the Young's inequality**

We invoke the Young's inequality (see [29]) for the RHS of (26) as follows

$$-\frac{C^2}{3} (\mathbf{B} : \delta^{(k-1)} \boldsymbol{\sigma}, \delta^{(k)} p_h)_{\Omega} \leq \frac{C^2}{3} \left[\frac{1}{2} \|\mathbf{B} : \delta^{(k-1)} \boldsymbol{\sigma}\|_{\Omega}^2 + \frac{1}{2} \|\delta^{(k)} p_h\|_{\Omega}^2 \right] \quad (27)$$

In lieu of (27), we write (26) as

$$\begin{aligned} & \frac{C^2}{3} \|\mathbf{B} : \delta^{(k)} \boldsymbol{\sigma}\|_{\Omega}^2 + \frac{C^2}{3} \|\delta^{(k)} p_h\|_{\Omega}^2 + C \Delta t \|\boldsymbol{\kappa}^{-1/2} \delta^{(k)} \mathbf{z}_h\|_{\Omega}^2 + C(\delta^{(k)} \boldsymbol{\sigma} : \mathbb{D}^{-1} \delta^{(k)} \boldsymbol{\sigma})_{\Omega} \\ & + \left[\frac{1}{2} \|\delta^{(k)} \zeta\|_{\Omega}^2 - \frac{7}{2} \|\delta_p^{(k)} \zeta - \delta_p^{(k)} \phi^p\|_{\Omega}^2 - \frac{1}{2} \|\delta^{(k)} \phi^p\|_{\Omega}^2 - \frac{C}{3} (\mathbf{B} : \delta^{(k)} \boldsymbol{\sigma}, \delta^{(k)} \phi^p)_{\Omega} \right] \\ & \leq \frac{C^2}{6} \|\mathbf{B} : \delta^{(k-1)} \boldsymbol{\sigma}\|_{\Omega}^2 \end{aligned}$$

which can be written as

$$\begin{aligned} & \|\mathbf{B} : \delta^{(k)} \boldsymbol{\sigma}\|_{\Omega}^2 + \overbrace{\|\delta^{(k)} p_h\|_{\Omega}^2}^{\geq 0} + \overbrace{\frac{3}{C} \Delta t \|\boldsymbol{\kappa}^{-1/2} \delta^{(k)} \mathbf{z}_h\|_{\Omega}^2}^{\geq 0} + \overbrace{\frac{3}{C} (\delta^{(k)} \boldsymbol{\sigma} : \mathbb{D}^{-1} \delta^{(k)} \boldsymbol{\sigma})_{\Omega}}^{\geq 0} + \overbrace{\frac{3}{2C^2} \|\delta^{(k)} \zeta\|_{\Omega}^2}^{\geq 0} \\ & - \overbrace{\frac{3}{C^2} \left[\frac{7}{2} \|\delta_p^{(k)} \zeta - \delta_p^{(k)} \phi^p\|_{\Omega}^2 + \frac{1}{2} \|\delta^{(k)} \phi^p\|_{\Omega}^2 + \frac{C}{3} (\mathbf{B} : \delta^{(k)} \boldsymbol{\sigma}, \delta^{(k)} \phi^p)_{\Omega} \right]}^{\rightarrow 0} \leq \frac{1}{2} \|\mathbf{B} : \delta^{(k-1)} \boldsymbol{\sigma}\|_{\Omega}^2 \end{aligned}$$

□

3.2 Derivation of criterion

We desire to drive the following quantity to zero

$$\frac{3}{C^2} \left[\frac{7}{2} \|\delta_p^{(k)} \zeta - \delta_p^{(k)} \phi^p\|_{\Omega}^2 + \frac{1}{2} \|\delta^{(k)} \phi^p\|_{\Omega}^2 + \frac{C}{3} (\mathbf{B} : \delta^{(k)} \boldsymbol{\sigma}, \delta^{(k)} \phi^p)_{\Omega} \right] \quad (28)$$

Noting (24), we can write

$$\frac{C}{3} (\mathbf{B} : \delta^{(k)} \boldsymbol{\sigma}, \delta^{(k)} \phi^p)_{\Omega} = (\delta_p^{(k)} \zeta - \delta_p^{(k)} \phi^p, \delta^{(k)} \phi^p)_{\Omega} \quad (29)$$

Using (29), we can write (28) as

$$\frac{3}{C^2} \left[\frac{7}{2} \|\delta_p^{(k)} \zeta - \delta_p^{(k)} \phi^p\|_{\Omega}^2 + \frac{1}{2} \|\delta^{(k)} \phi^p\|_{\Omega}^2 + (\delta_p^{(k)} \zeta - \delta_p^{(k)} \phi^p, \delta^{(k)} \phi^p)_{\Omega} \right]$$

which can also be written as

$$\frac{3}{C^2} \left[\frac{7}{2} \|\delta_p^{(k)} \zeta - \delta_p^{(k)} \phi^p\|_{\Omega}^2 + \frac{1}{2} \|\delta_p^{(k)} \phi^p\|_{\Omega}^2 + (\delta_p^{(k)} \zeta - \delta_p^{(k)} \phi^p, \delta_p^{(k)} \phi^p)_{\Omega} \right]$$

which, given that $\delta_f^{(k)} \phi^p$ (see Appendix B), can also be written as

$$\frac{3}{2C^2} \left[6 \|\delta_p^{(k)} \zeta - \delta_p^{(k)} \phi^p\|_\Omega^2 + \|\delta_p^{(k)} \zeta\|_\Omega^2 \right]$$

which, in lieu of (4) and (6), can also be written as

$$\frac{3}{2C^2} \left[6 \|\alpha : \delta_p^{(k)} \epsilon^e\|_\Omega^2 + \|\alpha : \delta_p^{(k)} \epsilon^e + \beta : \delta_p^{(k)} \epsilon^p\|_\Omega^2 \right]$$

As a result, we pose the convergence criterion as

$$6 \|\alpha : \delta_p^{(k)} \epsilon^e\|_\Omega^2 + \|\alpha : \delta_p^{(k)} \epsilon^e + \beta : \delta_p^{(k)} \epsilon^p\|_\Omega^2 \leq TOL \quad (30)$$

where $TOL > 0$ is a pre-specified tolerance and represents a small value.

4 Results and conclusions

We derived the convergence criterion for a staggered solution algorithm for anisotropic poroelastoplasticity coupled with single phase flow. We applied the principle of contraction mapping which states that the difference of iterates monotonically reduces with coupling iterations for convergence to be achieved at each time step. The convergence criterion is designed such that the statement of contraction mapping holds true.

A Discrete variational statements

In lieu of (5), we write mass conservation equation as

$$\begin{aligned} \frac{\partial}{\partial t} (Cp + \frac{C}{3} \mathbf{B} : \boldsymbol{\sigma} + \phi^p) + \nabla \cdot \mathbf{z} &= q \\ C \frac{\partial p}{\partial t} + \nabla \cdot \mathbf{z} &= q - \frac{C}{3} \mathbf{B} : \frac{\partial \boldsymbol{\sigma}}{\partial t} - \frac{\partial \phi^p}{\partial t} \end{aligned} \quad (31)$$

The discrete in time form of (31) in the $(n+1)^{th}$ time step is written as

$$C \frac{1}{\Delta t} (p^{k,n+1} - p^n) + \nabla \cdot \mathbf{z}^{k,n+1} = q^{n+1} - \frac{1}{\Delta t} \frac{C}{3} \mathbf{B} : (\boldsymbol{\sigma}^{k,n+1} - \boldsymbol{\sigma}^n) - \frac{1}{\Delta t} (\phi^{p^{k,n+1}} - \phi^{p^n})$$

where Δt is the time step. The fixed stress split constraint implies that $\boldsymbol{\sigma}^{k,n+1}$ gets replaced by $\boldsymbol{\sigma}^{k-1,n+1}$ as $\boldsymbol{\sigma}$ is fixed during the flow solve. The modified equation is written as

$$C(p^{k,n+1} - p^n) + \Delta t \nabla \cdot \mathbf{z}^{k,n+1} = \Delta t q^{n+1} - \frac{C}{3} \mathbf{B} : (\boldsymbol{\sigma}^{k-1,n+1} - \boldsymbol{\sigma}^n) - (\phi^{p^{k,n+1}} - \phi^{p^n})$$

As a result, the discrete weak form of mass conservation is given by

$$\begin{aligned} C(p_h^{k,n+1} - p_h^n, \theta_h)_\Omega + \Delta t (\nabla \cdot \mathbf{z}_h^{k,n+1}, \theta_h)_\Omega + (\phi^{p^{k,n+1}} - \phi^{p^n}, \theta_h)_\Omega \\ = \Delta t (q^{n+1}, \theta_h)_\Omega - \frac{C}{3} (\mathbf{B} : (\boldsymbol{\sigma}^{k-1,n+1} - \boldsymbol{\sigma}^n), \theta_h)_\Omega \end{aligned}$$

The weak form of the linear momentum balance is given by

$$(\nabla \cdot \boldsymbol{\sigma}, \mathbf{q})_\Omega + (\mathbf{f} \cdot \mathbf{q})_\Omega = 0 \quad (\forall \mathbf{q} \in \mathbf{U}(\Omega)) \quad (32)$$

where $\mathbf{U}(\Omega)$ is given by

$$\mathbf{U}(\Omega) \equiv \{ \mathbf{q} = (u, v, w) : u, v, w \in H^1(\Omega), \mathbf{q} = \mathbf{0} \text{ on } \Gamma_D^p \}$$

where $H^m(\Omega)$ is defined, in general, for any integer $m \geq 0$ as

$$H^m(\Omega) \equiv \{w : D^\alpha w \in L^2(\Omega) \ \forall |\alpha| \leq m\},$$

where the derivatives are taken in the sense of distributions and given by

$$D^\alpha w = \frac{\partial^{|\alpha|} w}{\partial x_1^{\alpha_1} \dots \partial x_n^{\alpha_n}}, \quad |\alpha| = \alpha_1 + \dots + \alpha_n,$$

We know from tensor calculus that

$$(\nabla \cdot \boldsymbol{\sigma}, \mathbf{q})_\Omega \equiv (\nabla, \boldsymbol{\sigma} \mathbf{q})_\Omega - (\boldsymbol{\sigma} : \nabla \mathbf{q})_\Omega \quad (33)$$

Further, using the divergence theorem and the symmetry of $\boldsymbol{\sigma}$, we arrive at

$$(\nabla, \boldsymbol{\sigma} \mathbf{q})_\Omega \equiv (\mathbf{q}, \boldsymbol{\sigma} \mathbf{n})_{\partial\Omega} \quad (34)$$

We decompose $\nabla \mathbf{q}$ into a symmetric part $(\nabla \mathbf{q})_s \equiv \frac{1}{2}(\nabla \mathbf{q} + (\nabla \mathbf{q})^T) \equiv \boldsymbol{\epsilon}^e(\mathbf{q})$ and skew-symmetric part $(\nabla \mathbf{q})_{ss}$ and note that the contraction between a symmetric and skew-symmetric tensor is zero to obtain

$$\boldsymbol{\sigma} : \nabla \mathbf{q} \equiv \boldsymbol{\sigma} : (\nabla \mathbf{q})_s + \cancel{\boldsymbol{\sigma} : (\nabla \mathbf{q})_{ss}}^0 = \boldsymbol{\sigma} : \boldsymbol{\epsilon}^e(\mathbf{q}) \quad (35)$$

From (32), (33), (34) and (35), we get

$$(\boldsymbol{\sigma} \mathbf{n}, \mathbf{q})_{\partial\Omega} - (\boldsymbol{\sigma} : \boldsymbol{\epsilon}^e(\mathbf{q}))_\Omega + (\mathbf{f}, \mathbf{q})_\Omega = 0$$

which, after invoking the traction boundary condition, results in the discrete weak form

$$(\mathbf{t}^{n+1}, \mathbf{q}_h)_{\Gamma_N^p} - (\boldsymbol{\sigma}^{k,n+1} : \boldsymbol{\epsilon}^e(\mathbf{q}_h))_\Omega + (\mathbf{f}^{n+1}, \mathbf{q}_h)_\Omega = 0$$

B Change in plastic porosity over flow solve is zero

To understand why $\delta_f^{(k)} \epsilon^p = 0$ and hence $\delta_f^{(k)} \phi^p = 0$, we present the basic algorithmic framework for the solution of elastoplastic equations: The system of equations (2) is first solved with $\gamma = 0$ for a trial stress state $\boldsymbol{\sigma}^{\text{trial}}$.

- ✓ If $\Phi(\boldsymbol{\sigma}^{\text{trial}}) \leq 0$, then we proceed with $\boldsymbol{\sigma} = \boldsymbol{\sigma}^{\text{trial}}$.
- ✓ If $\Phi(\boldsymbol{\sigma}^{\text{trial}}) > 0$, then the system (2) is solved with $\gamma > 0$ thereby lending us plastic strain. The procedure to solve (2) with $\gamma > 0$ is referred to as a return mapping algorithm [30–38]. The solution $\boldsymbol{\sigma}^{\text{return map}}$ of the return mapping algorithm is such that $\Phi(\boldsymbol{\sigma}^{\text{return map}}) = 0$ and we proceed with $\boldsymbol{\sigma} = \boldsymbol{\sigma}^{\text{return map}}$.

In summary, the solution $\boldsymbol{\sigma}$ is such that $\Phi(\boldsymbol{\sigma}) \leq 0$. During the subsequent flow solve, since the stress tensor is fixed, the value of the yield function does not change i.e. $\Phi(\boldsymbol{\sigma}) \leq 0$ still. This implies that $\gamma = 0$ during the flow solve and the porous solid does not accumulate any plastic strain during the flow solve.

References

- [1] Wolfgang Bangerth, Ralf Hartmann, and Guido Kanschat. deal. ii—a general-purpose object-oriented finite element library. *ACM Transactions on Mathematical Software (TOMS)*, 33(4):24–es, 2007.
- [2] Anders Logg, Kent-Andre Mardal, and Garth Wells. *Automated solution of differential equations by the finite element method: The FEniCS book*, volume 84. Springer Science & Business Media, 2012.
- [3] Christophe Prud’Homme, Vincent Chabannes, Vincent Doyeux, Mourad Ismail, Abdoulaye Samake, and Gonalo Pena. Feel++: A computational framework for galerkin methods and advanced numerical methods. In *ESAIM: Proceedings*, volume 38, pages 429–455. EDP Sciences, 2012.

- [4] Michael A Heroux, Roscoe A Bartlett, Vicki E Howle, Robert J Hoekstra, Jonathan J Hu, Tamara G Kolda, Richard B Lehoucq, Kevin R Long, Roger P Pawlowski, Eric T Phipps, et al. An overview of the trilinos project. *ACM Transactions on Mathematical Software (TOMS)*, 31(3):397–423, 2005.
- [5] Frédéric Hecht. New development in freefem++. *Journal of numerical mathematics*, 20(3-4):251–266, 2012.
- [6] Benjamin S Kirk, John W Peterson, Roy H Stogner, and Graham F Carey. libmesh: a c++ library for parallel adaptive mesh refinement/coarsening simulations. *Engineering with Computers*, 22(3):237–254, 2006.
- [7] Robert Anderson, Julian Andrej, Andrew Barker, Jamie Bramwell, Jean-Sylvain Camier, Jakub Cervený, Veselin Dobrev, Yohann Doudouit, Aaron Fisher, Tzanio Kolev, et al. Mfem: A modular finite element methods library. *Computers & Mathematics with Applications*, 81:42–74, 2021.
- [8] Bořek Patzák. Oofem—an object-oriented simulation tool for advanced modeling of materials and structures. *Acta Polytechnica*, 52(6), 2012.
- [9] François Faure, Christian Duriez, Hervé Delingette, Jérémie Allard, Benjamin Gilles, Stéphanie Marchesseau, Hugo Talbot, Hadrien Courtecuisse, Guillaume Bousquet, Igor Peterlik, et al. Sofa: A multi-model framework for interactive physical simulation. In *Soft tissue biomechanical modeling for computer assisted surgery*, pages 283–321. Springer, 2012.
- [10] Dominique Chapelle, J-F Gerbeau, J Sainte-Marie, and IE Vignon-Clementel. A poroelastic model valid in large strains with applications to perfusion in cardiac modeling. *Computational Mechanics*, 46(1):91–101, 2010.
- [11] Stephen C Cowin. Bone poroelasticity. *Journal of biomechanics*, 32(3):217–238, 1999.
- [12] Saumik Dana, Benjamin Ganis, and Mary F. Wheeler. A multiscale fixed stress split iterative scheme for coupled flow and poromechanics in deep subsurface reservoirs. *Journal of Computational Physics*, 352:1–22, 2018.
- [13] Saumik Dana. System of equations and staggered solution algorithm for immiscible two-phase flow coupled with linear poromechanics. *arXiv preprint arXiv:1912.04703*, 2019.
- [14] Saumik Dana, Joel Ita, and Mary F Wheeler. The correspondence between voigt and reuss bounds and the decoupling constraint in a two-grid staggered algorithm for consolidation in heterogeneous porous media. *Multiscale Modeling & Simulation*, 18(1):221–239, 2020.
- [15] Saumik Dana and Mary F Wheeler. An efficient algorithm for numerical homogenization of fluid filled porous solids: part-i. *arXiv preprint arXiv:2002.03770*, 2020.
- [16] Saumik Dana, Xiaoxi Zhao, and Birendra Jha. Two-grid method on unstructured tetrahedra: Applying computational geometry to staggered solution of coupled flow and mechanics problems. *arXiv preprint arXiv:2102.04455*, 2021.
- [17] S. Dana and M. F. Wheeler. Convergence analysis of fixed stress split iterative scheme for anisotropic poroelasticity with tensor biot parameter. *Computational Geosciences*, 22(5):1219–1230, 2018.
- [18] S. Dana and M. F. Wheeler. Convergence analysis of two-grid fixed stress split iterative scheme for coupled flow and deformation in heterogeneous poroelastic media. *Computer Methods in Applied Mechanics and Engineering*, 341:788–806, 2018.
- [19] S. Dana. *Addressing challenges in modeling of coupled flow and poromechanics in deep subsurface reservoirs*. PhD thesis, The University of Texas at Austin, 2018.
- [20] Mohamad Jammoul, Mary F. Wheeler, and Thomas Wick. A phase-field multirate scheme with stabilized iterative coupling for pressure driven fracture propagation in porous media. *Computers & Mathematics with Applications*, 2021.
- [21] Mohamad Jammoul, Benjamin Ganis, and Mary F. Wheeler. General semi-structured discretization for flow and geomechanics on diffusive fracture networks. In *SPE Reservoir Simulation Conference*. Society of Petroleum Engineers, 2019.
- [22] Erlend Storvik, Jakub W Both, Kundan Kumar, Jan M Nordbotten, and Florin A Radu. On the optimization of the fixed-stress splitting for biot’s equations. *International Journal for Numerical Methods in Engineering*, 120(2):179–194, 2019.
- [23] Jakub W Both and Uwe Köcher. Numerical investigation on the fixed-stress splitting scheme for biot’s equations: Optimality of the tuning parameter. In *European Conference on Numerical Mathematics and Advanced Applications*, pages 789–797. Springer, 2017.

- [24] Maurice A Biot. Mechanics of deformation and acoustic propagation in porous media. *Journal of applied physics*, 33(4):1482–1498, 1962.
- [25] AH-D Cheng. Material coefficients of anisotropic poroelasticity. *International journal of rock mechanics and mining sciences*, 34(2):199–205, 1997.
- [26] AW Skempton. The pore-pressure coefficients a and b. *Geotechnique*, 4(4):143–147, 1954.
- [27] Olivier Coussy. *Poromechanics*. John Wiley & Sons, 2004.
- [28] M. A. Biot and D. G. Willis. The Elastic Coefficients of the Theory of Consolidation. *Journal of Applied Mechanics*, 24(4):594–601, 2021.
- [29] J Michael Steele. *The Cauchy-Schwarz master class: an introduction to the art of mathematical inequalities*. Cambridge University Press, 2004.
- [30] Antonin Settari and Dale A Walters. Advances in coupled geomechanical and reservoir modeling with applications to reservoir compaction. *Spe Journal*, 6(03):334–342, 2001.
- [31] Zhijun Liu and Ruijie Liu. A fully implicit and consistent finite element framework for modeling reservoir compaction with large deformation and nonlinear flow model. part i: theory and formulation. *Computational Geosciences*, 22(3):623–637, 2018.
- [32] JC Simo and G Meschke. A new class of algorithms for classical plasticity extended to finite strains. application to geomaterials. *Computational mechanics*, 11(4):253–278, 1993.
- [33] Ali Karrech, Klaus Regenauer-Lieb, and Thomas Poulet. A damaged visco-plasticity model for pressure and temperature sensitive geomaterials. *International journal of engineering science*, 49(10):1141–1150, 2011.
- [34] MR Salari, S a Saeb, KJ Willam, SJ Patchet, and RC Carrasco. A coupled elastoplastic damage model for geomaterials. *Computer methods in applied mechanics and engineering*, 193(27-29):2625–2643, 2004.
- [35] CD Foster, RA Regueiro, Arlo F Fossum, and Ronaldo I Borja. Implicit numerical integration of a three-invariant, isotropic/kinematic hardening cap plasticity model for geomaterials. *Computer Methods in Applied Mechanics and Engineering*, 194(50-52):5109–5138, 2005.
- [36] JC Simo and RL Taylor. A return mapping algorithm for plane stress elastoplasticity. *International Journal for Numerical Methods in Engineering*, 22(3):649–670, 1986.
- [37] Juan C Simo. Algorithms for static and dynamic multiplicative plasticity that preserve the classical return mapping schemes of the infinitesimal theory. *Computer Methods in Applied Mechanics and Engineering*, 99(1):61–112, 1992.
- [38] Eduardo A de Souza Neto, Djordje Peric, and David RJ Owen. *Computational methods for plasticity: theory and applications*. John Wiley & Sons, 2011.